ELSEVIER

Physica C 352 (2001) 77–81

PHYSICA C

www.elsevier.nl/locate/physc

Andreev resonances in quantum ballistic transport in SNS junctions

Å. Ingerman [a,*], J. Lantz [a], E. Bratus' [b], V. Shumeiko [a], G. Wendin [a]

[a] *Chalmers University of Technology and Göteborg University, 41296 Göteborg, Sweden*
[b] *B.Verkin Institute for Low Temperature Physics and Engineering, 310164 Kharkov, Ukraine*

Abstract

We report the results of an investigation of the effect of the superconducting bound states on coherent multiple Andreev reflections in quantum SNS junctions. A rich resonant structure of the current, associated with the bound states and consisting of peaks, onsets and oscillations, is found by numerical calculations. Positions of the current structures are not given by subharmonics of the energy gap but rather determined by the junction geometry. We present analytical classification of the resonant current structures and calculate their positions and amplitudes. We show that the resonant current structures in three-terminal SNS interferometers can be controlled by external magnetic flux.

PACS: 74.50.+r; 74.80.Fp; 74.20.Fg; 73.23.Ad
Keywords: Voltage biased Josephson junction; Multiple Andreev reflection; SNS junction; Ballistic transport; Mesoscopic superconductivity

Ballistic SNS junctions are interesting mesoscopic structures where the effect of Andreev bound states on the current transport can be accurately studied. Recent experiments on ballistic SNS junctions fabricated with high mobility 2DEG [1–4] revealed unusual features in the voltage dependence of the differential resistance, which were tentatively attributed to Andreev resonances. Such features have been observed neither in metallic break junctions nor in diffusive SNS junctions. The current in metallic break junctions is accurately described by the theory of coherent multiple Andreev reflections (MAR) [5,6] where the effect of Andreev bound states is completely neglected. This description is adequate because of the small (atomic) size of these junctions. In 2DEG devices, the junction size is typically comparable to the superconducting coherence length, and the Andreev bound states are well developed. This will lead to pronounced resonant features in the multiparticle currents. On the other hand, in diffusive junctions, the Andreev bound levels are washed out into a continuum spectrum and the current resonances diminish to the level of mesoscopic fluctuations (incoherent MAR).

We present a study of the effect of Andreev bound states on the current transport in ballistic SNS junctions. We will focus on quantum junctions where the resonant effects are most pronounced, however, the results can be extended to plane junctions with large number of weakly coupled

* Corresponding author.
E-mail address: ingerman@fy.chalmers.se (Å. Ingerman).

0921-4534/01/$ - see front matter
PII: S0921-4534(00)01698-1

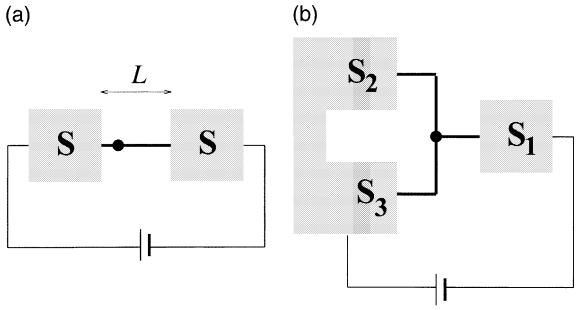

Fig. 1. Schematic configuration of SNS junctions: (a) two-terminal junction: the N-region consists of a quantum wire of length L with a single conducting channel; the bold dot indicates an impurity with transparency D; (b) three-terminal junction: the transparency of the connection point is D in the horizontal direction and D_1 in the vertical direction; the position of the Andreev levels is controlled by the the phase difference ϕ between terminals 2 and 3.

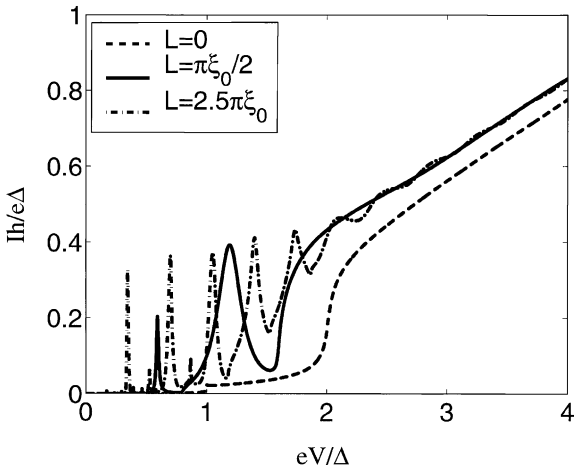

Fig. 2. IVC of the two-terminal junction (Fig. 1a) with the scatterer (impurity) symmetrically positioned at the center of the junction, transparency is $D = 0.1$; the temperature is zero.

conducting channels by integration over the conducting channels.

The junctions under consideration consist of a normal conducting quantum wire or a network of quantum wires (Fig. 1) connected to the superconducting electrodes. Experimentally, such structures can be realized, e.g., with the split-gated ballistic 2DEG confined between the superconducting electrodes. We will consider two types of junctions: a two-terminal SNS junction with a finite length $L \sim \xi_0 = \hbar v_F/\Delta$ and transparency D introduced by a scatterer in the quantum wire (Fig. 1a), and a three-terminal SNS-interferometer [7,8] (1b) with equipotential electrodes 2 and 3. The Andreev bound levels in the interferometer are controlled, in the limit of small coupling to electrode 1, $D \ll 1$, by applying a phase difference between the electrodes 2 and 3. The current–voltage characteristics (IVC) of the two-terminal junctions are presented in Fig. 2. The IVCs were numerically computed by using the theory of coherent MAR developed in Refs. [9,10] for junctions with strong electron–hole dephasing in the normal region (long SNS junctions, resonant junctions, etc.). For simplicity, the results are presented for symmetric junctions with the impurity positioned at the center of the normal wire. The following features of the current should be noted: (i) the current in finite-length junctions is considerably enhanced compared to the current in junctions of zero length, particularly in the subgap voltage region $eV < 2\Delta$; (ii) the main current onset in the junction with one Andreev level ($L = \pi\xi_0/2$) is shifted from $eV = 2\Delta$ towards smaller voltage; (iii) there are full-scale current peaks at subgap voltage, the number of peaks increasing with the junction length; (iv) there are no appreciably large peaks at small voltage; (v) the current shows oscillations above $eV = 2\Delta$. To interpret this complex behavior, we split the total current into partial multi-particle currents [9–11],

$$I(V) = \sum_n I_n(V)\theta(neV - 2\Delta),$$

and investigate n-particle currents separately.

The IVC of the single-particle current is presented in Fig. 3. The onset of the current at $eV = 2\Delta$, which is slightly washed out in a short junction ($L \ll \xi_0$), is completely suppressed in finite-length junctions. This gives rise to considerable current deficiency at large voltage. A small current onset appears in the junction with length $L = 2\pi\xi_0$. To explain this behavior, we derived an asymptotical form for the single particle current in the limit of small transparency $D \ll 1$,

$$I_1(V) = \frac{2eD}{h}\int_{\Delta-eV}^{-\Delta} \mathrm{d}E\, N(E)N(E+eV). \qquad (1)$$

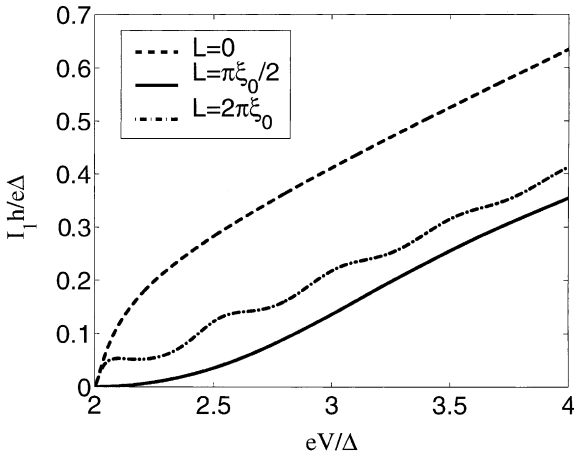

Fig. 3. Single-particle current in two-terminal junctions with different lengths, transparency $D = 0.1$; the current onset is appreciably suppressed, and current oscillations develop.

The current in Eq. (1) has the standard form of the tunnel single particle current where $N(E) = E\xi/[E^2 - \Delta^2\cos^2(EL/\hbar v_F)]$, $(\xi^2 = E^2 - \Delta^2)$ is the tunnel density of states (DOS) earlier calculated for proximity SN sandwiches [12]. The function $N(E)$ is constructed with the amplitudes of the scattering state wave functions, and it is constant within the N-region. The energy dependence of the DOS $N(E)$ is presented in Fig. 4: in junctions with arbitrary length, the DOS turns to zero at the gap

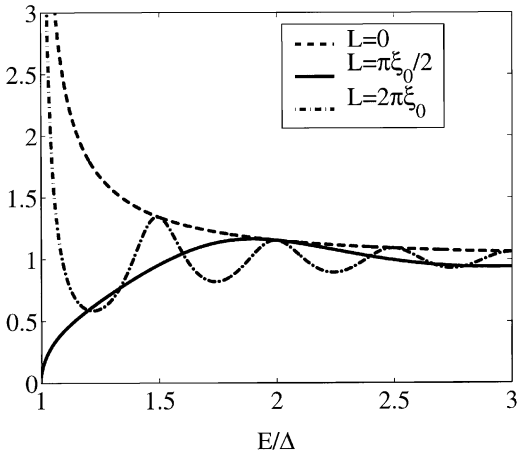

Fig. 4. Tunnel DOS $N(E)$ in the single-particle current (1). The DOS turns to zero at the gap edge except for junctions with length $L/\xi_0 = n\pi$ when a bound level splits from the continuum.

edge, except of the junctions with the length $L = n\pi\xi_0$ where the bound levels appear at the gap edge and where the DOS becomes singular. The oscillations of the DOS are related to the quasi-bound levels in the continuum (the Rowell–McMillan oscillations [13]). These properties of the DOS provide clear explanation of the properties of the single-particle current seen in Fig. 3.

The two-particle current is dominated by the resonant MAR processes shown in Fig. 5a. The asymptotic formula for the two-particle current in the limit of $D \ll 1$ reads

$$I_2(V) = \frac{2e}{h}\int_{\Delta-2eV}^{-\Delta} \mathrm{d}E\ \frac{D^2 N_0 N_2}{4\sin^2\chi(E_1) + D^2\left(\frac{N_0+N_2}{2}\right)^2}, \tag{2}$$

where $N_n = N(E_n)$, $E_n = E + neV$, and $\chi(E) = (EL/\hbar v_F) - \arccos(E/\Delta)$. This equation has the form of a resonant current with the resonances coinciding with the position of the de Gennes–Saint-James levels in the SNI quantum well, $\sin\chi(E_1) = 0$ [14]. The current therefore has resonant onsets at the voltages $eV = \Delta + E_A^{(m)} < 2\Delta$, where $E_A^{(m)} > 0$ is the position of the mth bound level. The height of the onsets is of the order D. The resonant onset of the pair current in the junction with $L = \pi\xi_0/2$ (one bound level) is seen in Fig. 2 as a shifted onset of the main current. The width of the resonances in Eq. (2) is periodically modulated by the oscillation in the DOS $N(E)$. This modulation produces the oscillation features on the IVC clearly seen in Fig. 6.

Despite of the fact that the pair current is large, $\sim D$, the excess current of the junction is small, $\sim D^2$, similar to the atomic-size point contacts. This is the result of the fine cancellation of large pair current by the reduced single particle current at $eV \gg 2\Delta$.

We notice that in our calculations, the Andreev bound levels are not involved in the single-particle transport: the single-particle transport is non-resonant. According to the scattering theory scheme the states of the continuum spectrum in the electrodes are the reservoirs while the true bound states with zero width are disconnected from the reservoirs. Thus the single particle transport through the bound states is strictly forbidden.

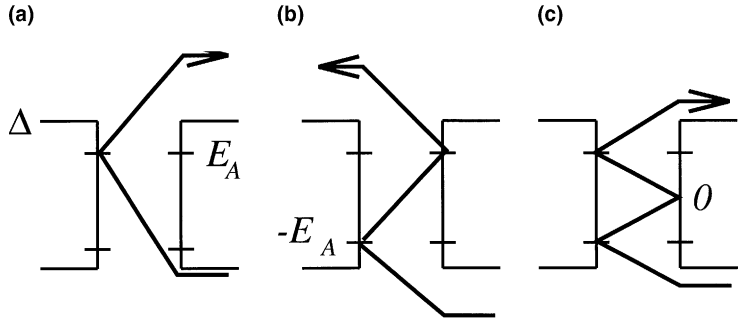

Fig. 5. Resonant MAR diagrams for (a) two-particle, (b) three-particle, and (c) four-particle currents.

Such an argumentation in fact relies upon the assumption about the small intrinsic width of the levels ($\sim\tau_i^{-1}$) compared to the level broadening ($\sim D\Delta$) due to the second order MAR processes, i.e., $\tau_i^{-1} \ll D\Delta$ (τ_i is the inelastic relaxation time).

The dominant contribution to the three- and four-particle currents results from the overlap of two Andreev resonances (see the MAR diagrams in Fig. 5b and c). The double resonance occurs at the voltage $eV = E_A^{(k)} + E_A^{(m)} > 2\Delta/3$ for the three-particle current, and $eV = (E_A^{(k)} + E_A^{(m)})/2 > \Delta/2$, for the four-particle current, and it is manifested by a current peak. The maximum transmissivity of the double resonance is equal to unity, which yields the height of the current peak of the order D, i.e. it is comparable to the resonant pair current. The IVC for the three-particle current is shown in Fig. 7. The double resonance current peaks of both the three- and four-particle currents are clearly seen in Fig. 2.

At the voltage $eV \ll \Delta/2$, the height of the current peaks decays exponentially. This is true even for long junctions if their transparency is small ($D \ll 0.1$): the Andreev spectrum is not commensurate with the equidistant sideband ladder, and higher order (triple, etc.) resonances do not exist.

The three-terminal SNS junction shown in Fig. 1b gives interesting possibilities for controlling the resonant features on the IVC. In this junction, a single Andreev bound level exists even in the limit of zero length of the normal wire, when a phase

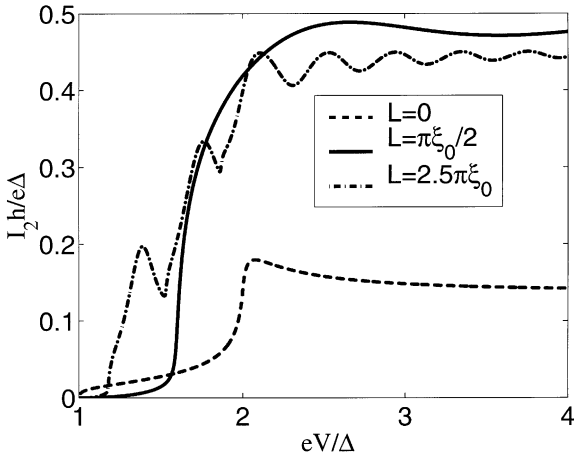

Fig. 6. The two-particle current shows resonant onsets at $\Delta < eV < 2\Delta$ due to the Andreev bound levels, accompanied by current oscillations due to the periodic modulation of the DOS; transparency $D = 0.1$.

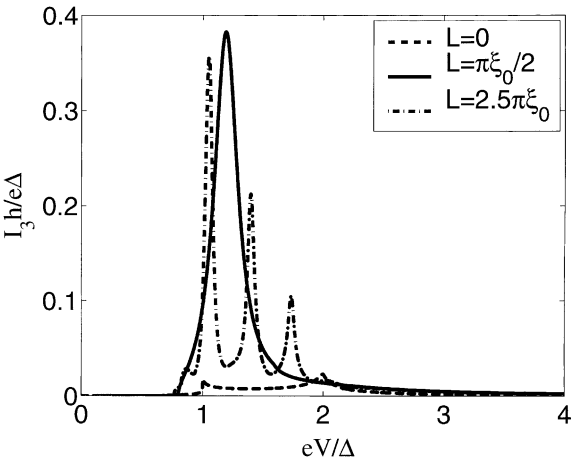

Fig. 7. Resonant peaks of the three-particle current: $D = 0.1$.

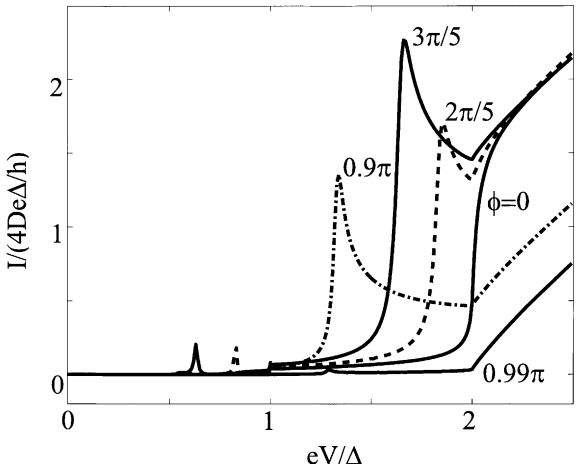

Fig. 8. IVCs of the three-terminal junction of Fig. 1b for different superconducting phases between the terminals 2 and 3: transparency $D = 0.02$, $D_1 = 0.9$.

difference is applied between the terminals 2 and 3. The theory for three-terminal junctions is developed in a similar way as the theory for the two-terminal junctions by combining the terminals 2 and 3 into a complex terminal with effective Andreev reflection. In the small transparency limit of the injection circuit, $D \ll 1$, the effective DOS of the complex terminal (2 and 3) has the form, $N(E) = E\xi/(E^2 - E_A^2)$, where $E_A = \Delta(1 - D_1 \sin^2(\phi/2))^{1/2}$ is the Andreev level energy, while the DOS of the simple terminal (1) is $N(E) = E/\xi$. The IVC of such a junction is shown in Fig. 8 for different phase differences ϕ. For $\phi = 0$ the terminals 2 and 3 work as a simple terminal, and the IVC is the same as in the non-resonant point contacts [2]. With the increase of the phase difference, the single particle current onset diminishes, while the resonant onset of the pair current instead develops, which leads to the shift of the position of the main current onset from $eV = 2\Delta$ to $eV = \Delta + E_A$. The tooth-like overshoot at the current onset is partly due to an onset resonance in the two-particle current and partly due to a double resonance in the three-particle current. At this voltage, the Andreev resonance at the complex terminal overlaps with the quasi-resonance at the gap edge of the simple terminal (see Fig. 5b), i.e. a double resonance. There is also a peak of the four-particle current at $eV = E_A$ due to the double Andreev resonance at the complex terminal (Fig. 5c). When the phase difference approaches $\phi = \pi$, all the multi-particle currents are suppressed and only the single particle current survives. This is due to the complete blockade of the Andreev reflections at the complex terminal at $\phi = \pi$, a property well known for the SN Andreev interferometers [15,16].

Acknowledgements

This work has been supported by research grants from KVA, NFR (Sweden) and NEDO International Joint Research Grant (Japan).

References

[1] H. Takayanagi, et al., Phys. Rev. B 51 (1995) 1374.
[2] A. Chrestin, et al., Phys. Rev. B 55 (1997) 8457.
[3] J. Kutchinsky, et al., Phys. Rev. Lett. 78 (1997) 931.
[4] G. Bastian, et al., Phys. Rev. Lett. 81 (1998) 1686.
[5] E. Scheer, et al., Phys. Rev. Lett. 78 (1997) 3535.
[6] B. Ludoph et al., Phys. Rev. B 61 (2000) 8561.
[7] A. Dimoulas, et al., Phys. Rev. Lett. 74 (1995) 602.
[8] J. Kutchinsky, et al., Phys. Rev. Lett. 83 (1999) 4856.
[9] G. Johansson, et al., Phys. Rev. B 60 (1999) 1382.
[10] G. Johansson, et al., Superlatt. Microstr. 25 (1999) 905.
[11] E. Bratus', et al., Phys. Rev. Lett. 74 (1995) 2110.
[12] E.L. Wolf, Principles of Electron Tunneling Spectroscopy, Oxford, 1985.
[13] J.M. Rowell, W.L. McMillan, Phys. Rev. Lett. 16 (1966) 453.
[14] P.G. de Gennes, D. Saint-James, Phys. Lett. 4 (1963) 151.
[15] H. Nakano, H. Takayanagi, Phys. Rev. B 47 (1993) 7986.
[16] F. Hekking, Yu. Nazarov, Phys. Rev. Lett. 71 (1993) 1625.